

RESEARCH

Open Access



Green synthesis of silver nanoparticles using Keratinase from *Pseudomonas aeruginosa*-C1M, characterization and applications as novel multifunctional biocatalyst

Marium Saba^{1,2}, Safia Farooq¹, Abdulrahman H. Alessa³, Kadriye Inan Bektas², Ali Osman Belduz², Alam Zeb Khan^{1,2}, Aamer Ali Shah¹, Malik Badshah¹ and Samiullah Khan^{1*}

Abstract

Introduction This study explores the biogenic synthesis of silver nanoparticles (AgNPs) using keratinase from *Pseudomonas aeruginosa*-C1M as a reducing and stabilizing agent. The synthesis of AgNPs was characterized by a color change from transparent to dark brown and a UV-Vis absorption peak at 450 nm, confirming nanoparticle formation. The study further investigates the structural, morphological, and functional properties of these AgNPs, particularly their antibacterial activity and their potential role in azo dye decontamination.

Methods and results The FTIR confirmed that AgNPs nanoparticles formation with keratinase. X-ray diffraction analysis showed that the prepared AgNPs were crystalline in nature and had face-centered cubic lattice planes. When observed under the transmission electron microscope and scanning electron microscope the nanoparticles were monodispersed spheres of different sizes. The diameter of the AgNPs was ~ 119 nm according to dynamic light scattering. High dispersion, long-term stability and excellent colloidal properties were supported by a high negative zeta potential value. The silver nanoparticles were found to have an antibacterial activity with zone of inhibition 25 mm and 33 mm against pathogenic strains of *Staphylococcus aureus* and *Escherichia coli* respectively. The synthesized zero-valent silver nanoparticles assisted in the decontamination of azo dyes (methyl red, methyl orange, safranin O and methyl violet) through the incorporation of sodium borohydride and light-catalyzed processes.

Conclusion This study demonstrates, for the first time, that keratinase from *Pseudomonas aeruginosa*-C1M can be used for AgNPs synthesis. The biogenic AgNPs exhibited potent antibacterial activity and played a crucial role in detoxifying hazardous azo dyes. These findings highlight the dual-functional potential of AgNPs for applications in antimicrobial treatments and environmental remediation. Future studies should explore their mechanism of action, scalability, and industrial applications.

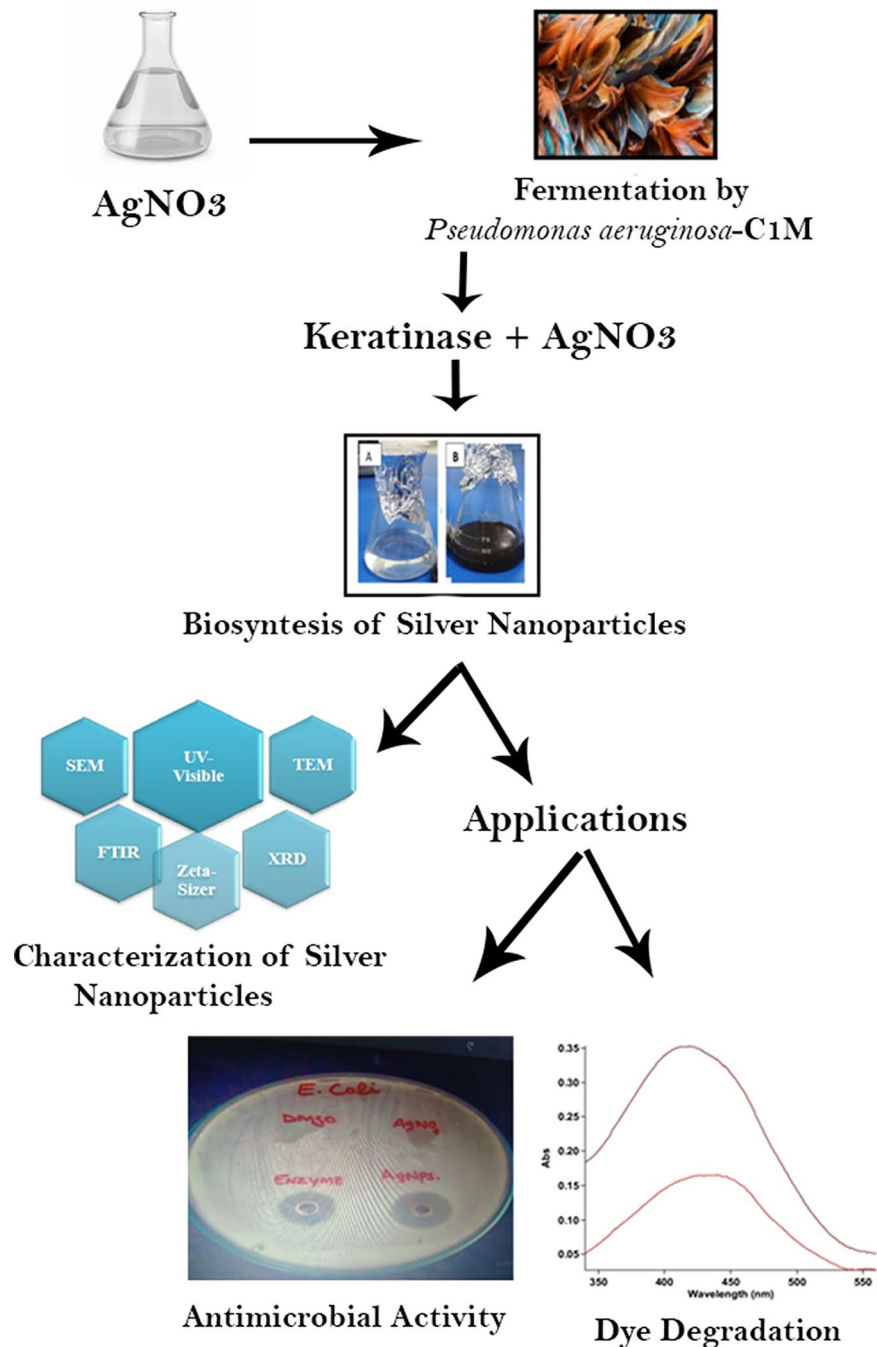
*Correspondence:
Samiullah Khan
samikhan@qau.edu.pk

Full list of author information is available at the end of the article



© The Author(s) 2025. **Open Access** This article is licensed under a Creative Commons Attribution-NonCommercial-NoDerivatives 4.0 International License, which permits any non-commercial use, sharing, distribution and reproduction in any medium or format, as long as you give appropriate credit to the original author(s) and the source, provide a link to the Creative Commons licence, and indicate if you modified the licensed material. You do not have permission under this licence to share adapted material derived from this article or parts of it. The images or other third party material in this article are included in the article's Creative Commons licence, unless indicated otherwise in a credit line to the material. If material is not included in the article's Creative Commons licence and your intended use is not permitted by statutory regulation or exceeds the permitted use, you will need to obtain permission directly from the copyright holder. To view a copy of this licence, visit <http://creativecommons.org/licenses/by-nc-nd/4.0/>.

Graphical abstract



Keywords Microbial keratinase, Biogenic synthesis, Nanoparticles, Antimicrobial, Dye decontamination

Introduction

With the convergence of nanotechnology and biology, a new field known as nano-biotechnology has emerged, combining molecular motors, nano-bio materials, nanocrystals, and biochips with inter-disciplinary biotechnology and nanotechnology techniques. The primary goal

of synthesizing and stabilizing various metallic and non-metallic nanoparticles is to give them unique properties to be employed in various fields. The key constraints for the novel properties of nanoparticles include their shape and size [1]. Noble metal nanoparticles are more appealing and have beneficial uses in different industries like

cancer therapy, electro-catalyst, photo-catalysts batteries, etc [2]. Due to increased surface area in nanoparticles that improve the characteristics of noble metals, enormous applications are possible [3].

Among them are also included silver nanoparticles. They are 100 nm consist of 20–15,000 silver atoms per particle, which hold distinguished chemical, physical, and biological attributes, contrasting their primary materials. Better physicochemical properties and thermal and electrical conductivity increased AgNP's potential among other noble metals. AgNP's exclusive behavior exhibited in biological activity makes them a promising candidate for antiviral, anti-inflammatory, antibacterial, and anti-cancer activities [4]. Lately, synthesized silver nanoparticles have been used as an alternate replacing conventional antibiotic agent [5].

Furthermore, AgNPs can captivate visible light, and they can also regulate the electron density [6]. Hence, they could be used as an appropriate medium for detecting surface-enhanced Raman scattering (SERS) and could analyze sensitive molecules [7].

In addition, ease of design and reproducibility for the methods used in silver nanoparticle synthesis can be used in several domains of life where novel properties are required. Many techniques, including heating, laser, and radiolysis, can synthesize AgNPs. The problem is that these methods are hazardous and expensive due to the involvement of harmful reducing agents and toxic solvents. Therefore, biogenic synthesis has been a viable option for the last few years to fulfill the green approach and proved to be sustainable [8]. Plants and their extracts, bacteria, fungi, and their secondary metabolites all have been employed in the past to produce AgNPs successfully.

The biosynthesis method using bacteria and their metabolites, especially extracellular enzymes, is a compassionate alternative to reduce the consequences of the consumption of chemicals involved in traditional methods. Furthermore, biogenic methods based on bacterial enzymes have huge potential and are more efficient and valuable than other biological substitutes because of simplicity of use, easy culturing, low cost and maintenance [9]. In this scenario, approaches to apply a single chemical to stabilize and act as reducing agent for controlling the growth process and meritoriously alter the size of the NPs are highly demanded. Due to this reason now, methodology has shifted towards developing a sustainable process for the biosynthesis of metallic NPs according to desired applications.

In an eco-friendly manner, silver nanoparticles can be used to decontaminate organic and inorganic dyes. Generally, it is common to utilize organic dyes in sectors ranging from plastic to paper to pharmaceuticals. Environment and aquatic bodies might be at risk from them.

Organic dyes like methyl orange and Congo red are frequently utilized in industries [10]. Before the expulsion of industrial waste, complete removal of dyes is essential since dyes are remarkably stable in water due to their complex structure. Green techniques for eliminating dyes from the environment might be possible in the presence of sunlight and catalyst [11].

In addition, transition metal's nanoparticles, such as silver, are responsible for the photo-degrading the organic dyes. Metals have desirable photo-electronic characteristics and ions on their surface and massive surface-to-mass ratios can cause their nanoparticle photocatalytic activities to be significantly higher. Silver nanoparticles have shown significant photocatalytic activity under UV-visible irradiation [12]. Photocatalysis is possible with silver nanoparticles because the absorption of visible light results in energizing conduction of electrons, as a result they are excited from their ground state to higher levels of energy, allowing them to participate in chemical processes. The dispersion of silver nanoparticles on supporting materials results in reduction of agglomeration [13]. In contrast to the metal oxide nanoparticles such as TiO₂, silver nanoparticles can have a modest number of charges, especially the one formed by the reducing the metal ions. Charging nanoparticles with functional groups like amino (–NH₂) groups can produce coordination connections between them and their supporting materials, minimizing particle detachment.

Understanding the efficiency of noble silver nanoparticles and the outcome of hazardous dyes to the ecosystem, the current study is based on green technology for synthesizing silver nanoparticles to investigate their antimicrobial and dye degradation activity. The sustainable approach is adopted using native keratinase of *Pseudomonas aeruginosa*-C1M, and the in-situ bio-reduction processes of silver ions into silver nanoparticles are effectively achieved without externally adding any capping agent. Native keratinase of *Pseudomonas aeruginosa*-C1M, used for the proposed work, possesses keratinolytic activity and is involved in the degradation of hard-to-degrade proteinaceous substrates into peptides and amino acids. Leather bioprocessing, pharmaceuticals, dehairing of hides, nitrogen fertilizer manufacture, and feed formulation all employ keratinases to some extent [14]. However, keratinases' potential to generate metallic nanoparticles has only been used in a few pieces of research [15].

In this study, we report the synthesis of well-defined silver nanoparticles produced by keratinase of *Pseudomonas aeruginosa*-C1M and characterization of silver nanoparticles carried out through several techniques, like UV-Vis spectroscopy, XRD, SEM, TEM, FT-IR, and DLS, emphasize the novelty of keratinase *Pseudomonas aeruginosa*-C1M for the formation of stable AgNPs.

Further, antimicrobial and dye degradation properties of silver nanoparticles were also explored.

This study offers a novel method, by using *Pseudomonas aeruginosa*-C1M keratinase for the first time in the biogenic synthesis of silver nanoparticles (AgNPs). In addition to their strong antibacterial activities, these keratinase-capped AgNPs are effective at degrading variety of hazardous azo dyes into less dangerous forms. This dual purpose demonstrates the potential of AgNPs produced from keratinase in biomedical and environmental applications.

Materials and methods

Biosynthesis of silver nanoparticles

In this study, keratinolytic strain *Pseudomonas aeruginosa*-C1M was used [16]. Keratinase production was done using a Feather Basal medium (FBM) under submerged fermentation. For the prospective keratinase production, the flask was seeded with *Pseudomonas aeruginosa*-C1M and kept at 37°C for 48 h. at shaking conditions of (200 rpm). After 15 min of centrifugation at 3,000 g and 4°C, the culture supernatant was stored at -20°C for later use as crude keratinase. Moreover, to confirm that keratinase was involved for AgNPs synthesis, because protein hydrolysate found in the supernatant of keratinase consists of peptides and amino acids [17] resulting from keratin breakdown, which may also have a role in AgNPs formation [18], partially purified keratinase (60% ammonium sulfate precipitation 25U/mg) was also employed for the biogenic synthesis of keratinase.

Silver nitrate solution and crude keratinase served as precursors for the synthesis of AgNPs. 50 ml of a solution of 2 mM AgNO₃ solution was combined with 5 ml of crude keratinase (14U/mg followed by continuous stirring for 24 h. at room temperature. A 2mM AgNO₃ solution devoid of crude keratinase was utilized as a negative control. The change of color in reaction mixture was observed and AgNPs were purified after centrifugation at 10,000 rpm for 15 min at temperature 4°C. Subsequently, the pellet was suspended in sterilized double distilled water. The following approaches were used to characterize eco-friendly silver nanoparticles.

Characterization of silver nanoparticles

UV-visible spectrophotometry

A common method for determining the creation and properties of nanoparticles is UV-visible spectroscopy. A UV-visible spectrophotometer was used to track the generation of Ag-NPs. Using a UV-visible spectrophotometer with an accuracy of 1 nm between the wavelength ranges of 300–800 nm [19], the absorbance was calculated, and the peak was analyzed to determine the wavelengths at which nanoparticles were synthesized (Varian Cary 100 Bio UV-Visible Spectrophotometer).

Scanning Electron Microscopy (SEM)

Using a scanning electron microscope (SEM) (ZEISS EVO LS10) with a working voltage of 25 kV, silver nanoparticles (AgNPs) were morphologically examined. On a carbon tape-coated stub, a few drops of biosynthesized AgNPs were applied. Additionally, the stub was sputter coated with gold to provide crisp pictures [20].

Transmission Electron Microscopy (TEM)

A drop of nanoparticle was placed on a copper grid with a mesh size of 200 and a 3.05 mm hexagonal form for transmission electron microscopy (Agar Scientific, Essex, UK) [21]. The coating was accomplished using samples suspended in chloroform. After 305 min of imaging, the surplus liquid was swept away, and the grids were air dried. The micrographs were taken with a JEM-1400 (JEOL, USA) at a voltage of 100 kV.

Dynamic light scattering (DLS) and zeta potential

DLS (dynamic light scattering) and zeta potential analysis on a zeta sizer were used to assess biosynthesized silver nanoparticles' size distribution, surface charge, and hydrodynamic diameter at ambient temperature (Malvern Instruments, ZS nano, UK) [22]. For analysis, freeze-dried materials were distributed in water. The set up was operated at 15 V/cm of electric field to examine the data by using Zeta Sizer.

Fourier transform infrared (FTIR) analysis

Functional groups on the surface of nanoparticles in the range 4000–400 cm⁻¹ were identified using Fourier-transform infrared (FTIR) spectroscopy (Jasco, FTIR 6300, Japan) [23] at a resolution of 4 cm⁻¹. The samples were prepared by using the freeze-drying technique.

X-ray diffraction (XRD)

Silver nanoparticles were examined using X-ray diffraction (XRD) to identify their crystalline structure. The XRD pattern was recorded using an EMPYREAN X-ray diffract meter running [24] at 45 kV and 40 mA current strength with Cu-K/radiation (= 1.5406). The diffracted intensities were measured at a scan rate of 0.5°/min from 5° to 90° 2 angles.

Applications for silver nanoparticles

Anti-bacterial activity assay

By using the traditional well diffusion approach, the antibacterial activity of the AgNPs against the pathogenic strains *Escherichia coli* ATCC 25,922 and *Staphylococcus aureus* ATCC 25,923 were assessed. Culture broths were placed onto Müller-Hinton agar plates, after test strains in nutrient broth had been incubated for 24 h. at 37°C and 200 rpm. Wells were drilled in the agar with a sterilized 5 mm cork borer, and 100 µl of AgNP solution was

decanted into each well. Additionally, antibacterial activity was determined using DMSO, crude keratinase, and sterilized distilled water as controls. The widths of the clear inhibitory zones were measured after 24 h. of incubation at 37°C to assess the antibacterial activity.

Dyes degradation by silver nanoparticles

Sodium borohydride catalyzed degradation of dye 1 ml of a 100 mM sodium borohydride solution was added to 1 ml of 0.15mM methyl red (MR) and methyl orange (MO) solutions. After diluting the solutions to 10 ml with deionized water, the reaction mixture was rapidly agitated for 5 min. Solutions were then supplemented with 2 ml of silver nanoparticle followed by agitation for 5 min. Dye degradation was evidenced by the solution becoming de-colored. Non-catalyzed reaction was used as a reference. The deteriorating process was observed using a UV-visible absorption spectrophotometer.

Photocatalytic degradation of dyes by silver nanoparticles In the presence of silver nanoparticles, methyl violet (MV) and safranin O (SO) dyes were selected for photocatalytic degradation. In a flask, 10 mL of dyes (0.15 mM) methyl violet and Safranin O were added separately. After adding 1 mg of AgNPs and thoroughly mixing with a magnetic stirrer, the reaction mixture was exposed to sunlight for 3 h. The kinetics of photocatalytic degradation of methyl violet and safranin O was investigated by observing the change in emission spectra of UV-visible absorption spectrophotometer.

Results and discussion

Biosynthesis of silver nanoparticles

As silver ions reduced to silver nanoparticles after 24 h., the appearance of dark brown nanoparticles demonstrated the synthesis of silver nanoparticles (Fig. 1). Crude keratinase was incubated with silver nitrate (AgNO₃) solution and after 2 h. color creation started, which indicated the visual confirmation of synthesis of silver nanoparticles. This is because microbial keratinase was responsible for capturing the metal ion (silver ion) and acting as a reductant to create silver nanoparticles [25]. Bio-reduction of silver ions was responsible for enhanced color intensity of biosynthesized nanoparticles. The control solution remained clear, while the production of dark brown to blackish particles confirmed the creation of silver nanoparticles (Fig. 2).

Microbial keratinase offers a biological and environmentally friendly substitute for chemical synthesis of AgNPs. Those who are biosynthesized have industrial, biomedical, and antibacterial uses. Producing nanoparticles with the right size and characteristics can be optimized by knowing the enzymatic mechanism. Further optimization research needs to be done. Numerous research has demonstrated that silver nanoparticles may be formed from bacteria and their metabolites. However, just a few publications exist on the production of AgNPs using keratinase. Lateef and colleagues said that they synthesized silver nanoparticles using *Bacillus safensis* keratinase [26]. Similarly, another study revealed that keratinase was accountable for the brown hue of silver nanoparticles [27]. Similarly, the reducing agent *Stenotrophomonas maltophilia* R13 keratinase was employed to synthesize AgNPs in an environmentally suitable

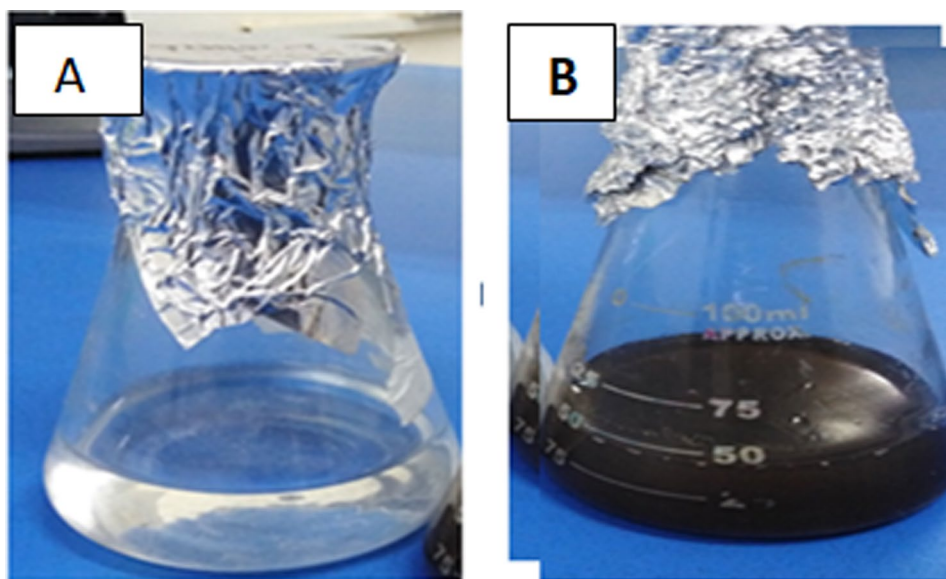
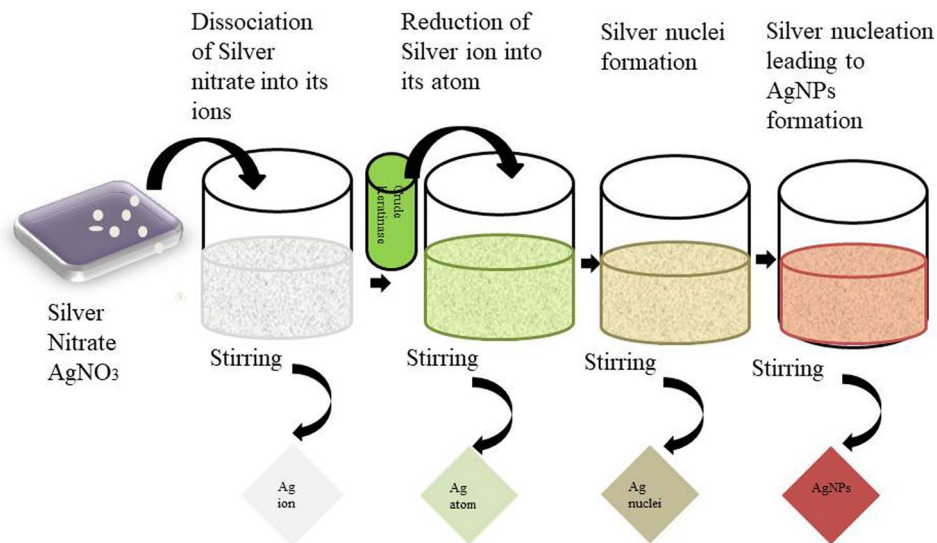


Fig. 1 Illustration of silver nanoparticle biosynthesis: (A) shows the control containing a silver nitrate solution, while (B) depicts the synthesized silver nanoparticles



Mechanism of silver nanoparticles AgNPs formation

Fig. 2 Schematic representation of the synthesis mechanism of crude keratinase-mediated silver nanoparticles (AgNPs) using AgNO_3 as a precursor. The enzymatic reduction of Ag^+ ions by crude keratinase leads to the formation of AgNPs. Key steps include the interaction of Ag^+ with crude keratinase, nucleation, and stabilization of AgNPs. Spectroscopic and morphological analyses confirm the successful synthesis and stability of AgNPs

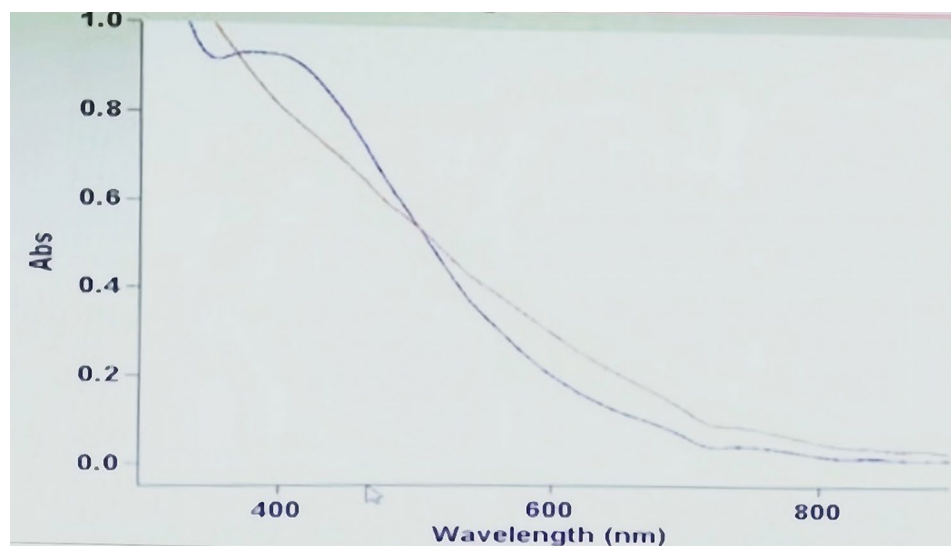


Fig. 3 UV-Vis absorption spectra of crude keratinase-mediated silver nanoparticles (AgNPs). The spectra exhibit a characteristic surface plasmon resonance (SPR) peak in the range of 400–450 nm, confirming the synthesis of AgNPs. The shift in peak intensity and position suggests variations in nanoparticle size, distribution, and stability. The red line indicates control (silver nitrate solution) while blue indicates peak of silver nanoparticles at 460 nm

manner [15]. Characterization revealed more details on the structure and properties of the silver nanoparticles. A range of silver nitrate concentrations (0.5 mM, 1 mM, 2 mM, 5 mM, 10 mM) was tested. 2 mM AgNO_3 was selected because it provided the best balance between nucleation, growth, and stability based on experimental optimization. Insufficient and excess silver ions may lead to improper nanoparticle yield. While 2mM AgNO_3 produces uniform, stable, and well-dispersed nanoparticles.

Characterization of silver nanoparticles

UV-visible spectroscopy

UV-visible spectrophotometers were used to induce localized surface plasmon resonance in metal, which results in the formation of an electric field and caused excitation of electrons. (Fig. 3) Resonance at a certain wavelength might result in beam scattering within that wavelength range. When Ag^+ ion is reduced from AgNP complex to Ag^0 ion by *Pseudomonas aeruginosa*-C1M

keratinase resulted in surface plasmon resonance. At 450–470 nm, a robust, single, and wide resonance peak was seen, demonstrating the biogenic production of AgNPs [28]. Furthermore, it was shown that AgNPs have a spherical shape because they only have one surface plasmon resonance peak [29], while anisotropic particles have several peaks. The new discovery is supported by earlier research on the creation of silver nanoparticles from fungus, which indicated a peak in the UV-Visible spectrum at 442 nm [30]. Meanwhile, Parkash and colleagues reported that a surface plasmon resonance peak at 420 nm was recorded, followed by a steady rise to 445 nm during a 48-hour period [31]. The UV-Visible spectrum of keratinase-mediated silver nanoparticles (AgNPs) may lack a sharp peak due to several reasons. Significant variation in size and shape, that is polydispersity, leads to the broadening of surface plasmon resonance (SPR) which in turn is responsible for non-sharp or diffuse peaks. Aggregation of AgNPs is also a factor for broad UV-Visible spectrum.

Another possible reason may be the keratinase, or other biomolecules present in the reaction mixture may adsorb onto the nanoparticle surface, altering the electronic environment and leading to a broader or less-defined peak. The dispersion medium and any residual reactants can affect the UV-Vis spectrum, causing peak broadening or even shifting.

Scanning Electron Microscopy (SEM)

Biogenic silver nanoparticles (AgNPs) were examined using SEM to assess their size and surface form. Silver nanoparticles were determined to be round, smooth, and ranging in size from 15 nm to 100 nm using SEM micrographs (Fig. 4). The AgNPs' predominant spherical shape is confirmed by the SEM micrographs, which is in line with other research on biologically produced silver nanoparticles. A non-uniform nucleation and growth

process, which can be impacted by variables like temperature, precursor concentration, and the type of biomolecules used in the synthesis, is suggested by the wide size distribution (15 nm to 100 nm).

This range includes the reported average size in comparable studies (33.75 nm and 35 nm), which supports the idea that the biological source and synthesis circumstances can affect the results of AgNP production.

Although images were collected at various magnifications, aggregation was also observed. One common artifact from sample preparation is the aggregation seen in SEM pictures. Nanoparticles may cluster because of capillary forces drawing them together when the stub dries. However, several scientists have already discovered that AgNPs vary in size [32]. Recently, in a study on the synthesis of AgNPs using the marine macroalgae *Padina sp.*, the average particle size determined by the standard error of the mean was 33.75 nm [31]. Meanwhile, another research discovered AgNPs to be 35 nm in diameter and spherical in form [33]. AgNPs' antimicrobial activity, catalytic, and optical properties are strongly influenced by their size and shape.

The surface area-to-volume ratios of smaller nanoparticles (less than 50 nm) are often higher, which increases their reactivity and possible biological activity.

Transmission Electron Microscopy (TEM)

Transmission electron micrographs of silver nanoparticles are presented in the image below (Fig. 5). AgNPs were discovered to be between 15 and 35 nm in average size and spherical in form. Kanan et al. estimated the size to be between 30 and 44 nm [34]. In contrast to this research, variations in synthesis conditions have an impact on nanoparticle size. These AgNPs' biological and catalytic properties, especially their antibacterial activity, are enhanced by their small size. Compared to other biogenic techniques, enzyme-mediated synthesis

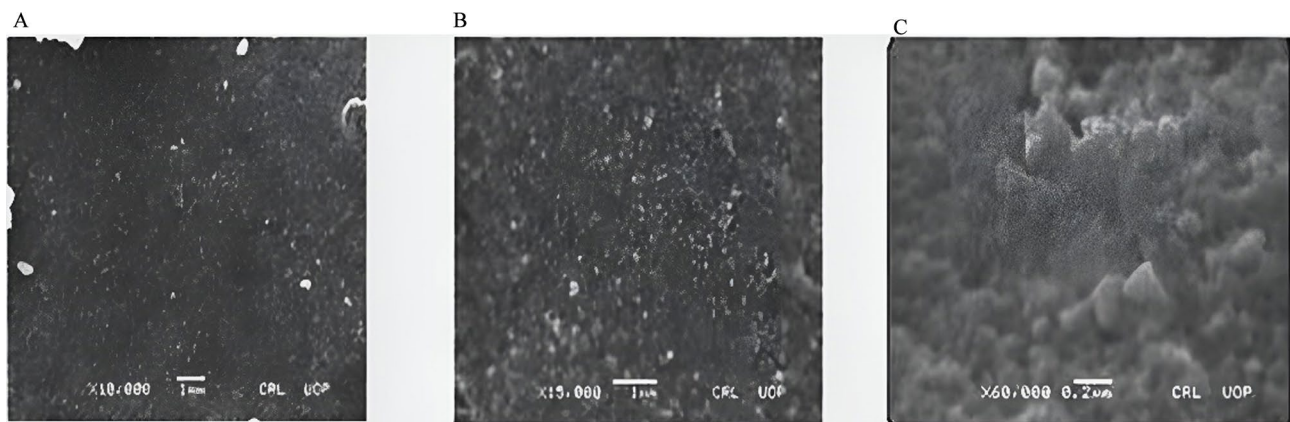


Fig. 4 Scanning Electron Microscopy (SEM) images of the sample at different magnifications. (A) Image at 10,000x magnification showing overall surface morphology with a scale bar of 1 µm. (B) Image at 15,000x magnification providing a closer view of the microstructure with a scale bar of 1 µm. (C) Image at 50,000x magnification revealing fine surface details and nanoparticle distribution with a scale bar of 0.2 µm



Fig. 5 Transmission electron micrographs of biogenically synthesized silver nanoparticles at various magnification (60X, 100X and 150X), **(A)** Low-magnification TEM image showing the overall morphology and dispersion of nanoparticles. **(B)** Higher magnification image displaying the internal structure and boundaries of the nanoparticles. **(C)** Further high-resolution TEM image revealing the atomic arrangement within the material

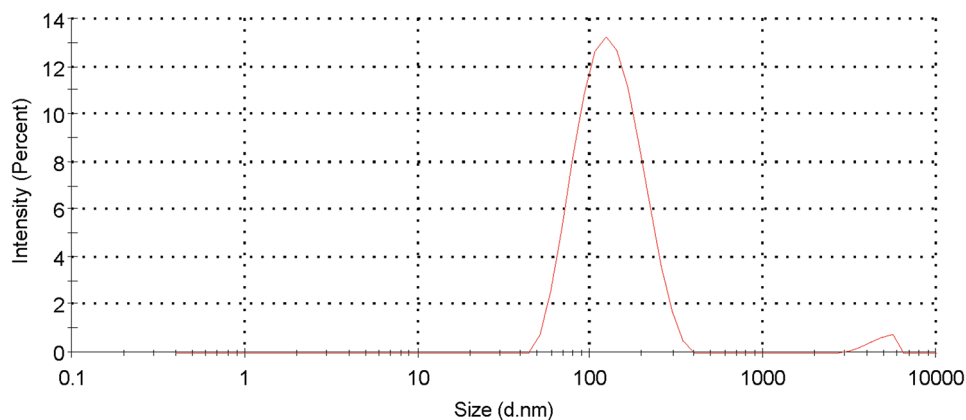


Fig. 6 Size distribution by intensity of silver nanoparticles synthesized using keratinase, showing a primary peak around **100 nm**, indicating the dominant nanoparticle population, with a minor peak suggesting possible aggregation or secondary particle formation

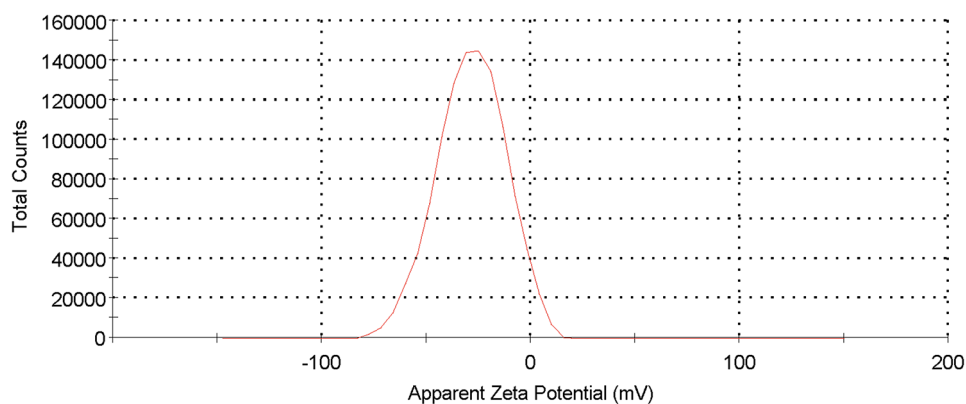


Fig. 7 Silver nanoparticles prepared with keratinase exhibit a negative zeta potential distribution, which suggests the existence of negatively charged capping agents that support nanoparticle stability by inhibiting aggregation

yields nanoparticles that are more homogeneous and evenly distributed. TEM offers a more precise picture of nanoparticle dispersion than SEM, demonstrating that keratinase efficiently stabilizes AgNPs to reduce aggregation.

Dynamic light scattering (DLS) and zeta potential

A fundamental aspect of nanoparticles is their size, which has a significant effect on their dissolution rate, physical

stability, saturation solubility, and their active performance. With a range of 20–400 nm, the average particle size was found to be 119.8 nm. AgNPs were found to have a polydispersity index (PDI) of 0.210, showing good dispersion of the nanoparticles. Additionally, charge was assessed using zeta potential, whose negative value indicates the presence of negatively charged capping agents that inhibit agglomeration. It is, nonetheless, implicated in the stability of colloidal systems (Figs. 6 and 7).

Moreover, divergence in findings of TEM and DLS is owing to fluctuation in sample circumstances. For dynamic light scattering (DLS) water based hydrodynamic system was employed whereas for TEM dry samples were used [35, 36]. In the literature, it has been noted that the size of silver nanoparticles varies with the reducing agent. According to recent research, the average size of AgNPs encapsulated in fungal chitosan was 75–80 nm; whereas AgNPs generated from *Trichoderma viride* had an average size assessed by zeta sizer of 242 nm but were well dispersed [37, 38].

Fourier transform infrared (FTIR) analysis

The bio-molecular mechanism responsible for the stability of biosynthesized nanoparticles were identified using FTIR measurements. The FTIR spectrum showed several distinct peaks. The NH_2 -amino-acidic group has a peak at 3268 cm^{-1} , which could be seen. At $2853\text{--}2963\text{ cm}^{-1}$, side chain vibrations of symmetric and anti-symmetric C–H stretching modes of aliphatic and aromatic groups were found. At a wavelength of 2500 cm^{-1} , the S–H bond was found to be present. While the peak at 1625 cm^{-1} reflected the C=O I bond, the peak at 1447 cm^{-1} demonstrated the carboxylic acid bending of the OH group. Similarly, the 1381 cm^{-1} peak revealed the aliphatic bending group of CHS and CH_2 . A peak at 1060 cm^{-1} indicated the presence of S=O. 623 cm^{-1} , on the other

hand, was previously assumed to be N–H stretched (Fig. 8).

It has been demonstrated in the past that free amine groups and cysteine residues are crucial for the efficient stabilization and capping of AgNPs by interacting proteins and nanoparticles. Along with the findings previously mentioned, it seems that protein and leftover chemicals played a role in the stability and capping of AgNPs.

X-ray diffraction (XRD)

The XRD pattern analysis revealed crystalline silver nanoparticles. The five diffraction peaks at 2θ values of 38.03° , 44.29° , 64.49° , 77.49° , and 81.51° indicate that the face-centered cubic structure of silver may be indexed to the (1 1 1), (2 0 0), (2 2 0), (3 1 1), and (2 2 2) reflection planes. Notably, the peak at 38.03° exhibited the highest intensity, indicating a strong preferential orientation along the (111) plane (Fig. 9). The presence of these peaks suggests that the AgNPs were successfully synthesized and stabilized by keratinase, a biomolecule that facilitated the reduction of silver ions, as supported by previous studies [39]. Similar findings have been reported where biosynthesized AgNPs exhibited identical diffraction peaks, confirming their crystalline FCC structure. Furthermore, the sharp and well-defined peaks indicate the high crystallinity of the nanoparticles, aligning with results from other studies on biogenic AgNP synthesis

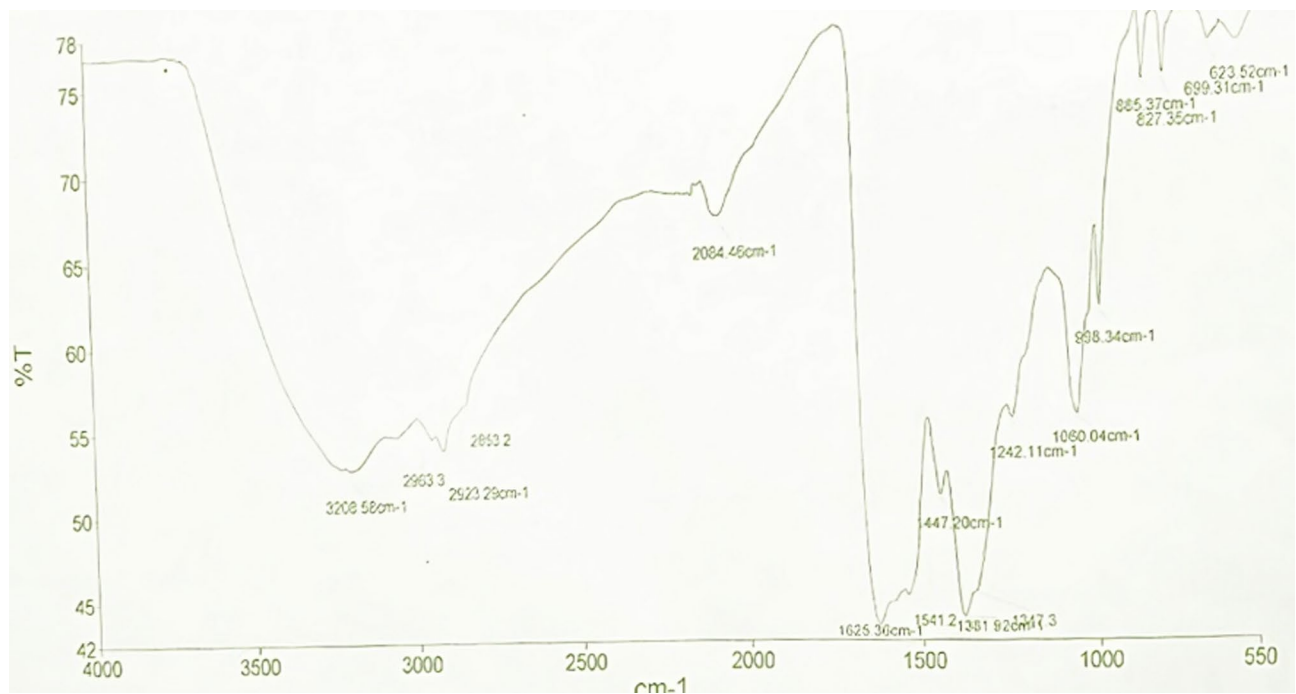


Fig. 8 FTIR spectrum of biogenic silver nanoparticles, displaying characteristic absorption bands. Peaks around $3200\text{--}2800\text{ cm}^{-1}$ correspond to O–H and C–H stretching vibrations, while bands near 1625 cm^{-1} and 1541 cm^{-1} indicate amide bonds. The peaks in the fingerprint region ($1242\text{--}600\text{ cm}^{-1}$) suggest the presence of sulfhydryl, aromatic, and aliphatic functional groups, confirming biomolecule capping on the nanoparticles

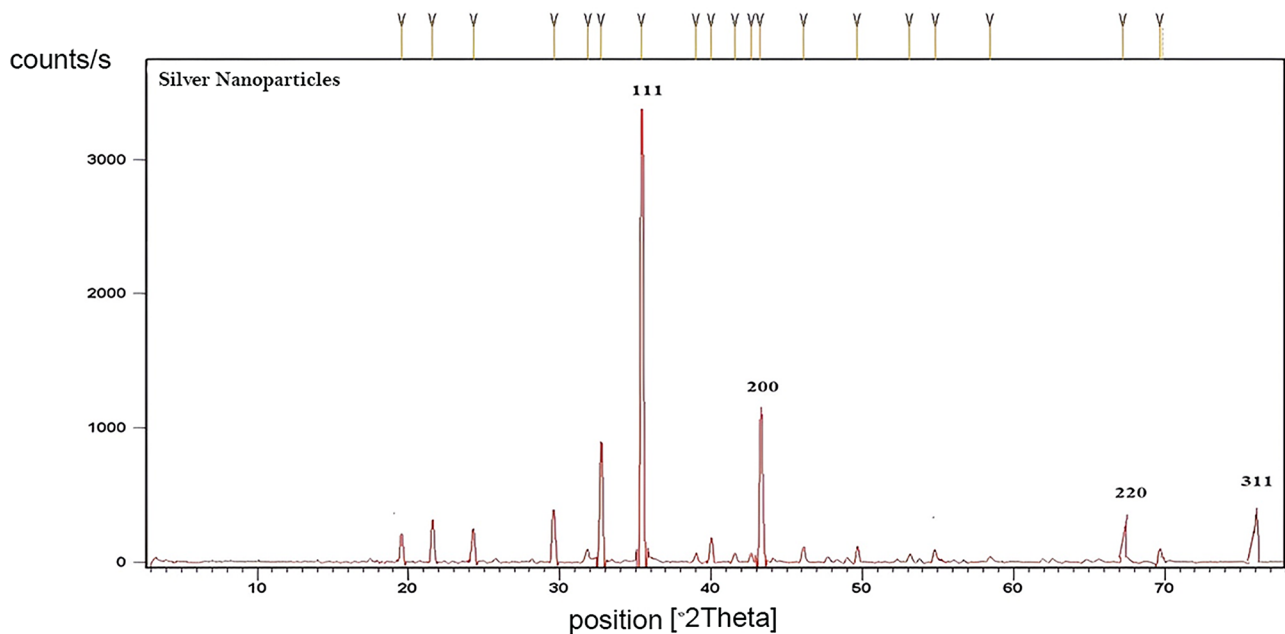


Fig. 9 XRD pattern of biogenic silver nanoparticles, showing characteristic diffraction peaks at 2θ values corresponding to the (111), (200), (220), and (311) crystallographic planes. These peaks confirm the face-centered cubic (FCC) crystalline structure of silver nanoparticles, consistent with the standard JCPDS reference pattern

Table 1 Zone of inhibition of antimicrobial activity of keratinase mediated silver nanoparticles

| S. No. | Pathogenic strain | Zone of inhibition |
|--------|------------------------------|--------------------|
| 1. | <i>E. coli</i> ATCC 25,922 | 33 mm |
| 2. | <i>S. aureus</i> ATCC 25,923 | 25 mm |

[40]. The use of keratinase in AgNP stabilization also suggests a green synthesis approach, reducing the need for toxic chemical reducing agents while ensuring nanoparticle stability. These findings contribute to the growing body of research on eco-friendly synthesis methods for AgNPs with potential biomedical and catalytic applications.

Application of biogenic silver nanoparticles

Antibacterial activity of silver nanoparticles

For testing the antibacterial properties of AgNPs produced from *Pseudomonas aeruginosa*-C1M keratinase, the well diffusion technique was used using a 100 micro liter nanoparticles solution. *Escherichia coli* ATCC 25,922 Gram-negative and gram-positive *Staphylococcus aureus* ATCC 25,923 had inhibition zones of 33 mm and 25 mm, respectively. Zone of inhibition of pathogenic strains are listed in Table 1. A class of proteases called keratinases may be responsible for the inhibitory function of keratinase, since it has been shown to limit the growth of microorganisms (Fig. 1 Supplementary).

AgNPs made by biosynthesis have been shown to be effective against *E. coli* [41]. In another study AgNPs from crude keratinase demonstrated effective inhibition

against distinct isolates of *E. coli* [42]. AgNPs have a proven high surface area to volume ratio, which makes them superior to bulk silver metal in terms of their exceptional antibacterial activity since it would enable tight attachment of these nanoparticles with microbial cells, enabling their antimicrobial effect to be size dependent [43]. Moreover, bactericidal mechanism involves: Release of Ag^+ ions, which disrupt bacterial cell membranes. Reactive oxygen species (ROS) formation, leading to oxidative stress and bacterial death. Electrostatic interactions between bacterial walls and positively charged ions, resulting in membrane rupture [44]. The antimicrobial activity observed in crude keratinase preparations is preferably due to the proteolytic activity of keratinase, that can lead to the disintegration of cell wall and membrane of microorganisms resulting into cell lysis and death. Moreover, another reason could be that the microbes that produce keratinases may also exude other antimicrobial substances. For example, secondary metabolites containing anti-microbial, which can be present in crude extract. Likewise, the synergistic effect of both; the existence of further antimicrobial compounds produced by the keratinase-producing microorganisms and proteolytic degradation of microbial structures is responsible for antimicrobial activity of crude keratinase [45]. Furthermore, AgNPs can interact closely with bacterial membranes because of their high surface-to-volume ratios. Bacterial cell death, ion leakage, and membrane damage are the results of interactions between the positively charged silver ions and the negatively charged

bacterial cell wall. Gram-positive bacteria exhibit greater sensitivity than Gram-negative bacteria due to differences in their cell wall structure. The chemistry behind photocatalysis of organic dye is because AgNPs promote electron transfer, which produces reactive species that break down organic dyes [46].

Dyes degradation by silver nanoparticles

Dyes, especially azo dyes, have a considerable impact on the environment, due to their toxicity, longevity, and intricate interactions with environmental conditions. The xenobiotic nature of dye effluents and their degradation compounds make natural remediation challenging and presents direct threats to aquatic and terrestrial environments. Furthermore, as azo dyes degrade, especially when their composition is changed by microbiological and physico-chemical processes, carcinogenic aromatic amines may be produced [47]. Environmental factors like light, moisture, and oxygen availability also impact on dye degradation and can occasionally result in a formation of hazardous byproducts in ecosystems. Alternatives to traditional treatment techniques, which are often expensive, energy-intensive, and produce hazardous sludge, are promising when it comes to sustainable remediation options, especially microbial technologies. However, biogenic nanoparticles are the promising entities for the degradation of dyes [48]. Generally, in dye degradation experiments it's observed that either the new peaks will emerge, or already existing peaks will disappear. Emergence of new peaks or disappearance of peak is correspondent to degradation product. But in some cases, like here, the degradation via keratinase mediated synthesized silver nanoparticles, only reduction in the primary peaks appear without the origination of new peaks. Several factors play their role in this regard: The degradation products may exhibit absorption bands that coincide with those of the original dye, leading to a general decrease in peak intensity without the emergence of distinct new peaks. In such scenarios, UV-Vis spectrophotometry might struggle to differentiate between the parent dye and its degradation products, and the phenomenon is known as Overlapping absorption bands. Another possible explanation for this is the complete mineralization of dye. After complete mineralization, dye convert into inorganic molecules like carbon dioxide (CO₂) and water (H₂O), and they do not have the capacity to absorb light in the UV-Visible spectrum. Subsequently, a decrease in the original peak occurs instead of the emergence of new peaks.

Another reason for this is either the rapid degradation of intermediates or their low concentration. The detection of intermediate products would be challenging if they degrade immediately after formation. It means that they might not build up to a certain detectable range,

which reduces the overall absorbance lacking formation of new peaks. In low concentrations, the intermediate products might be too delicate to observe, thus leading to the diminishing peaks of the original dye.

Sodium borohydride catalyzed degradation of dye (Methyl red and methyl orange)

In the present era, harmful industrial dyes are increasingly contaminating water sources, environmental conservation is a major concern in contemporary culture. The synthetic and non-biodegradable nature of many dyes, such as methyl orange (MO) and methyl red (MR), makes them a serious environmental hazard. These poisonous, mutagenic, and carcinogenic properties of dyes make them potentially harmful to human health and aquatic life [49].

Nanoparticles—in particular, silver nanoparticles (AgNPs) have drawn interest as catalysts in dye degradation due to their large surface area and increased catalytic activity [50]. One of the efficient ways to degrade methyl orange (MO) and methyl red (MR) is to reduce them by using sodium borohydride (NaBH₄). AgNPs act as an electron mediator to speed up the process and NaBH₄ act as a reducing agent, the reaction proceeds according to an electron transfer mechanism. High surface-to-volume ratio of biogenic nanoparticles offers more active sites for interaction with the dye molecules, responsible for their catalytic efficiency. Adsorption between MO molecules and silver nanoparticles may also be facilitated by a coating of reducing agent on the silver nanoparticles. Smaller particles have an advantage over larger ones in the oxidation-reduction reaction between active MO and NaBH₄.

The presence of AgNPs and NaBH₄ reduces methyl orange, an organic sulfosalt, and causes it to lose its distinctive 465 nm spectral band [51]. The following is an outline of the reaction mechanism:

- (1) $\text{Ag}/\text{NaBH}_4 + \text{h} \rightarrow \text{Ag}/\text{NaBH}_4 (\text{h} + \text{e}^-)$
- (2) $2\text{e}^- + \text{MOH} + \text{H}^+ \rightarrow \text{MOH}_2$
- (3) The 465 nm MO band began to go away over time.

An electron and a hole are expected to be involved in the reaction process, that is not yet completely understood

However, methyl red (MR) is an acid-base indicator whose absorption spectra are pH-dependent. The peak shift from 442 nm to 428 nm was noticed after the addition of NaBH₄ to methyl red solution. More hydroxyl ions are present, which causes a pH change. N=N-methyl red is converted to less hazardous form, which may be seen as a degradation peak. NaBH₄ in the presence of nano silver catalyzes the breakdown of dyes to nontoxic and smaller molecules via an electron transfer action between

nucleophilic BH_4^- ions and electrophilic organic dye molecules (Fig. 2 Supplementary).

Photo-catalytic degradation of dyes by silver nanoparticles (Safranin O and methyl violet)

Safranin O (SO) and Methyl violet (MV) dyes degraded when silver nanoparticles were present during photolysis studies under sunlight. Irradiation for 3 h caused the red hue of SO and MV dyes to fade. The degradation of SO and MV under used settings is indicative of a reduction in the absorption spectra of materials at the maximum wavelength of SO and MV dye (Fig. 3 Supplementary).

Expected mechanism for the photocatalysis of safranin O is as follows: A photon with energy of $h\nu$, which creates a hole (h^+) in the valence band, stimulates an electron in the valence band (e^-) to go into the conduction band. Finally, hydroxyl radicals were produced by trapping holes on the surface of the hydroxyl group. When oxygen dissolved in water reacts with electrons in the conduction band, superoxide radical anions $\text{O}_2^{\cdot-}$ are formed. Hydrogen radicals (HO^{\cdot}) were formed because of the protonation of superoxide anions $\text{O}_2^{\cdot-}$. Dye degradation was ultimately caused by the superoxide anions' activity. Color changes were induced by valence band holes and conduction band electrons, respectively. A photon with energy of $h\nu$, which creates a hole (h^+) in the valence band, stimulates an electron in the valence band (e^-) to go into the conduction band [52]. Because of SPR excitation, the photocatalytic activity of AgNPs may be described by their ability to absorb visible light and convert it into chemical energy.

Similarly, for the photocatalysis of Methyl violet (MV), the expected mechanism is as follows: AgNP act as photocatalyst for the degradation of methyl violet (MV) dye. The method breaks down organic contaminants by activating reactive species in response to light. Electronic transitions occur, in which the absorption energy is greater than the band gap energy of the photocatalyst. Electron-hole pairs (h^+VB) are created when electrons (e^-) in the valence band (VB) are stimulated to the conduction band (CB) by exposure to solar light. The dye molecules are broken down by hydroxyl radicals (OH^{\cdot}) and superoxide anions ($\text{O}_2^{\cdot-}$), which are produced because of redox processes facilitated by these charge carriers. The key reactions in the degradation process include:

1. Photoexcitation: AgNP absorbs visible light, generating electron-hole pairs.
2. Oxygen Reduction: Electrons in the CB react with O_2 , forming superoxide radicals ($\text{O}_2^{\cdot-}$).
3. Hydroxyl Radical Formation: Holes (h^+VB) oxidize water or hydroxide ions to produce OH^{\cdot} .

4. Methyl violet Degradation: Hydroxyl radicals and electron-hole pairs interact with MV, leading to its breakdown.
5. Redox Reactions: Electrons and holes directly participate in pollutant reduction and oxidation, forming degradation products [53].

The concept of photocatalysis and antibacterial potential is correlated. AgNPs show strong antibacterial potential. AgNPs along with ZnO enhance antibacterial efficacy by inducing production of reactive oxygen species (ROS), that ultimately lead towards oxidative stress and cell damage. Ag^+ ions take part in amplifying oxidative damage and nanoparticles prevent the biofilm formation. Thus, the synergistic effect of AgNP and ZnO improves antibacterial activity multiple times. AgNPs integrated into ZnO structures showed the ability to degrade photocatalytically. Through permeability enhancement and bacterial cell wall disruption, the ZnO-AgNP nanoparticles broke down bacterial biofilm [54]. Silver nanoparticles (AgNPs) exhibit cytotoxicity, which refers to their ability to cause damage or death to cells. The cytotoxic effects of AgNPs depend on various factors, including particle size, shape, concentration, surface charge, and exposure duration. AgNPs exert toxicity primarily through mechanisms such as oxidative stress, disruption of cellular membranes, mitochondrial dysfunction, DNA damage, and apoptosis induction [55]. They generate reactive oxygen species (ROS), which lead to oxidative damage, inflammation, and interference with cellular signaling pathways. Additionally, AgNPs can release silver ions (Ag^+), which contribute to their toxicity by interacting with proteins, enzymes, and genetic material inside cells. The extent of cytotoxicity varies across different cell types and is influenced by environmental conditions. While AgNPs have broad applications in medicine, coatings, and antimicrobial products, their potential adverse effects on human health and the environment necessitate careful evaluation and regulation [56].

Conclusion

This study presents an eco-friendly and cost-effective method for synthesizing protein-capped silver nanoparticles (AgNPs) using keratinase from *Pseudomonas aeruginosa*-C1M. Characterization techniques confirmed that the AgNPs are spherical, crystalline, and effectively bio-conjugated with keratinase. The synthesized AgNPs demonstrated significant antibacterial activity against various bacterial strains. However, further research is necessary to assess their cytotoxicity before considering biological or pharmaceutical applications.

Abbreviations

| | |
|------------------|-----------------------------------|
| AgNPs | Silver nanoparticles |
| FTIR | Fourier transform infrared |
| <i>S. aureus</i> | <i>Staphylococcus aureus</i> |
| <i>E. coli</i> | <i>Escherichia coli</i> |
| MR | Methyl red |
| MO | Methyl orange |
| SO | Safranin O |
| MV | Methyl violet |
| SERS | Surface-enhanced Raman scattering |
| XRD | X-ray diffraction |
| SEM | Scanning Electron Microscope |
| TEM | Transmission Electron Microscopy |
| DLS | Dynamic light scattering |
| DMSO | Dimethyl sulfoxide |
| PDI | Polydispersity Index |
| VB | Valence Band |
| CB | Conduction Band |

Supplementary Information

The online version contains supplementary material available at <https://doi.org/10.1186/s12896-025-00959-5>.

Supplementary Material 1

Acknowledgements

We are grateful to Molecular Biology lab at Karadeniz Technical University, Trabzon, Turkey for providing opportunities of analytical work. Higher Education Commission of Pakistan provided financial assistance to carry out this work (No: 9904/Federal/ NRPU/R&D/HEC/2017).

Author contributions

Marium Saba was involved in conceptualization, methodology, investigation, writing original draft, and formal analysis. Safia Farooq and Alam Zeb Khan performed the experiments and helped in writing the first draft of the manuscript. Abdulrahman H Alessa provided resources, reviewing the final draft and formatting the article. Kadriye Inan, Ali Osman Belduz, Malik Badshah and Aamer Ali Shah wrote the comments, review, and involved in supervision of the students. Samiullah Khan was the main supervisor, design the project and secured funding. All authors contributed to manuscript revision, read, and approved the manuscript.

Funding

Higher Education Commission of Pakistan provided financial assistance to carry out this work (No: 9904/Federal/ NRPU/R&D/HEC/2017).

Data availability

Data is provided within the manuscript or supplementary information files.

Declarations

Ethics approval and consent to participate

The ethical approval for this study was obtained from Bioethical Committee, Quaid-i-Azam University, Islamabad, Pakistan with the assigned No #BEC-FBS-QAU2017-31. Informed consent was obtained whenever required.

Consent for publication

Not applicable.

Competing interests

The authors declare no competing interests.

Author details

¹Department of Microbiology, Faculty of Biological Sciences, Quaid-i-Azam University, Islamabad 45320, Pakistan

²Department of Molecular Biology, Faculty of Sciences, Karadeniz Technical University, Trabzon 61080, Turkey

³Department of Biology, Faculty of Sciences, University of Tabuk, Tabuk, Saudi Arabia

Received: 16 November 2024 / Accepted: 18 March 2025

Published online: 11 April 2025

References

- Restrepo CV, Villa CC. Synthesis of silver nanoparticles, influence of capping agents, and dependence on size and shape: A review. *Environ Nanotechnol Monit Manag*. 2021;15:100428. <https://doi.org/10.1016/J.ENMM.2021.100428>.
- Abbas R, Luo J, Qi X, Naz A, Khan IA, Liu H, et al. Silver nanoparticles: Synthesis, structure, properties and applications. *Nanomaterials*. 2024;14(7):1425. <https://doi.org/10.3390/NANO14171425>
- Chen F, Yan TH, Bashir S, Liu JL. Synthesis of nanomaterials using top-down methods, *Advanced Nanomaterials and Their Applications in Renewable Energy*, Second Edition. 2022. p. 37–60. <https://doi.org/10.1016/B978-0-323-99877-2.00007-2>
- Arshad F, Naikoo GA, Hassan IU, Chava SR, El-Tanani M, Aljabali AA, et al. Bioinspired and green synthesis of silver nanoparticles for medical applications: A green perspective. *Appl Biochem Biotechnol*. 2023;196(6):3636–69. <https://doi.org/10.1007/S12010-023-04719-Z>
- Shi S, Ou X, Long J, Lu X, Xu S, Zhang L. Nanoparticle-based therapeutics for enhanced burn wound healing: A comprehensive review. *Int J Nanomedicine*. 2024;19:11213–33. <https://doi.org/10.2147/IJN.S490027>.
- Trivedi S, Srivastava A, Saxena D, Ali D, Alarifi S, Solanki VS, et al. Phytofabrication of silver nanoparticles by using *Cucurbita maxima* leaf extract and its potential anticancer activity and pesticide degradation. *Mater Technol*. 2025;40. <https://doi.org/10.1080/10667857.2024.2440907>.
- Nasr N, Shafi M, Zhao T, Ali R, Ahmad I, Khan M, Deifalla A, Ragab AE, Zahid Ansari M. A two-fold SPR-SERS sensor utilizing gold nanoparticles and graphene thin membrane as a spacer in a 3D composite structure. *Spectrochim Acta Mol Biomol Spectrosc*. 2024;304:123331. <https://doi.org/10.1016/J.SAA.2023.123331>.
- Thavamurugan S, Annamalai A, Narayanan M, Devan M, Manoharan N, Prabha AL. Green synthesis of silver nanoparticles using *Osbeckia Leschenaultiana* DC extract: Optimization of synthesis, biological activities, larvicidal activity and toxicity analysis. *Inorg Chem Commun*. 2024;169:113011. <https://doi.org/10.1016/J.INOCHE.2024.113011>.
- Jayakumar M, Prabhu SV, Nirmala C, Sridevi M, Rangaraju M, Jayakumar M, et al. Keratinase: A futuristic green catalyst and potential applications. In: *Value Added Products From Food Waste*. 2024. p. 207–30. https://doi.org/10.1007/978-3-031-48143-7_11
- Raj S, Singh H, Trivedi R, Soni V. Biogenic synthesis of AgNPs employing terminalia Arjuna leaf extract and its efficacy towards catalytic degradation of organic dyes. *Sci Rep*. 2020;10:9616. <https://doi.org/10.1038/s41598-020-66851-8>.
- Roy A, Bharadvaja N. Establishment of root suspension culture of *Plumbago zeylanica* and enhanced production of *Plumbagin*. *Ind Crops Prod*. 2019;137:419–27.
- Cheng D, Liu R, Hu K. Gold nanoclusters: Photophysical properties and photocatalytic applications. *Front Chem*. 2022;10:958626. <https://doi.org/10.3389/FCHEM.2022.958626/BIBTEX>.
- Akpmie KG, Conradie J. Efficient synthesis of magnetic nanoparticle-*Musa acuminata* peel composite for the adsorption of anionic dye. *Arab J Chem*. 2020;13:7115–31. <https://doi.org/10.1016/j.arabjc.2020.07.017>.
- Bhange K, Nath A, Singh N, Chaturvedi V, Bhatt R. Statistical optimization and prediction of significant nutritional factors for keratinase production by *Stenotrophomonas maltophilia* Kb2 and its application as dehairing agent. *Bioresour Technol Rep*. 2023;23:101541. <https://doi.org/10.1016/J.BITEB.2023.101541>.
- Jang E-Y, Son Y-J, Park S-Y, Yoo J-Y, Cho Y-N, Jeong S-Y, Liu S, Son H-J. Improved biosynthesis of silver nanoparticles using keratinase from *Stenotrophomonas maltophilia* R13: Reaction optimization, structural characterization, and biomedical activity. *Bioprocess Biosyst Eng*. 2018;41:381–93. <https://doi.org/10.1007/s00449-017-1873-0>.
- Saba M, Khan A, Ali H, Bibi A, Gul Z, Khan A, Rehman MMU, Badshah M, Hasan F, Shah AA, Khan S. Microbial pretreatment of chicken feather and its co-digestion with rice husk and green grocery waste for enhanced biogas production. *Front Microbiol*. 2022;13:792426. <https://doi.org/10.3389/FMICB.2022.792426/BIBTEX>.

17. Saba M, Akhter A, Ahmed H, Mehmood Z, Khan A, Saleh zada N, Badshah M, Hasan F, Shah AA, Khan S. Sustainable valorization of chicken feathers and grocery waste as organic fertilizer and its impact on yield and quality of spinach (*Spinacia oleracea*) plant. *Commun Soil Sci Plant Anal.* 2023;54:2995–3005. <https://doi.org/10.1080/00103624.2023.2253842>.
18. Ghodake G, Lim SR, Lee DS. Casein hydrolytic peptides mediated green synthesis of antibacterial silver nanoparticles. *Colloids Surf B Biointerfaces.* 2013;108:147–51. <https://doi.org/10.1016/J.COLSURFB.2013.02.044>.
19. Lateef A, Adelerie IA, Gueguim-Kana EB, Beukes LS, Matyumza N. Evaluation of feather hydrolysate-mediated silver nanoparticles as biofertilizers for the enhancement of vegetative growth and nutraceutical properties of vegetables. *Nanotechnol Environ Eng.* 2024;9:47–65. <https://doi.org/10.1007/S41204-023-00348-3/TABLES/7>.
20. Mohammed AM, Hassan KT, Hassan OM. Assessment of antimicrobial activity of chitosan/silver nanoparticles hydrogel and cryogel microspheres. *Int J Biol Macromol.* 2023;233:123580. <https://doi.org/10.1016/J.IJBIOMAC.2023.123580>.
21. Alves MF, Murray PG. Biological synthesis of monodisperse Uniform-Size silver nanoparticles (AgNPs) by fungal cell-free extracts at elevated temperature and pH. *J Fungi.* 2022;8:439. <https://doi.org/10.3390/JOF8050439>.
22. Salayová A, Bedlivočová Z, Daneu N, Baláz M, Lukáčová Bujňáková Z, Balázová L, Tkáčiková L. Green synthesis of silver nanoparticles with antibacterial activity using various medicinal plant extracts: Morphology and antibacterial efficacy. *Nanomaterials.* 2021;11:1005. <https://doi.org/10.3390/NANO11041005/S1>.
23. Oe T, Dechojarasri D, Kakinoki S, Kawasaki H, Furuike T, Tamura H. Microwave-assisted incorporation of AgNP into Chitosan–Alginate hydrogels for antimicrobial applications. *J Funct Biomater.* 2023;14:199. <https://doi.org/10.3390/JF14040199/S1>.
24. Takcı DK, Ozdenefe MS, Genc S. Green synthesis of silver nanoparticles with an antibacterial activity using *salvia officinalis* aqueous extract. *J Cryst Growth.* 2023;614:127239. <https://doi.org/10.1016/J.JCRYSGRO.2023.127239>.
25. Xin X, Qi C, Xu L, Gao Q, Liu X. Green synthesis of silver nanoparticles and their antibacterial effects. *Front Chem Eng.* 2022;4:941240. <https://doi.org/10.3389/FCENG.2022.941240/BIBTEX>.
26. Lateef A, Adelerie IA, Gueguim-Kana EB, Asafa TB, Beukes LS. Green synthesis of silver nanoparticles using keratinase obtained from a strain of *Bacillus safensis* LAU 13. *Int Nano Lett.* 2015;5:29–35. <https://doi.org/10.1007/s40089-014-0133-4>.
27. Sudha SSB, Sumathi SSS, Swabna VSV. Enzyme mediated synthesis and characterization of silver nanoparticles using keratinase enzyme producing micro-organisms. *Annals Phytomedicine: Int J.* 2020;9. <https://doi.org/10.21276/AP.2020.9.1.19>.
28. Vigneshwaran N, Ashtaputre N. Biological synthesis of silver nanoparticles using the fungus *Aspergillus flavus*. Elsevier; 2007.
29. Princy SSJ, Hentry C, Alodaini HA, Hatamleh AA, Arokiyaraj S, Bindhu MR. Hibiscus cannabinus seeds assisted spherical silver nanoparticles and its antibacterial and photocatalytic applications. *Chem Phys Impact.* 2023;6:100192. <https://doi.org/10.1016/J.CHPHI.2023.100192>.
30. Majeed S, Danish M, Binti Zahrudin AH, Dash GK. Biosynthesis and characterization of silver nanoparticles from fungal species and its antibacterial and anticancer effect. *Karbala Int J Mod Sci.* 2018;4:86–92. <https://doi.org/10.1016/j.kijoms.2017.11.002>.
31. Bhuyar P, Rahim MHA, Sundararaju S, Ramaraj R, Maniam GP, Govindan N. Synthesis of silver nanoparticles using marine macroalgae *Padina* Sp. and its antibacterial activity towards pathogenic bacteria. *Beni Suef Univ J Basic Appl Sci.* 2020;9:1–15. <https://doi.org/10.1186/s43088-019-0031-y>.
32. Phull A-R, Abbas Q, Ali A, Raza H, Kim SJ, Zia M, Haq I. Antioxidant, cytotoxic and antimicrobial activities of green synthesized silver nanoparticles from crude extract of *Bergenia ciliata*. *Futur J Pharm Sci.* 2016;2:31–6. <https://doi.org/10.1016/j.fjps.2016.03.001>.
33. Saravanan C, Rajesh R, Kaviarasan T, Muthukumar K, Kavitate D, Shetty PH. Synthesis of silver nanoparticles using bacterial exopolysaccharide and its application for degradation of azo-dyes. *Biotechnol Rep.* 2017;15:33–40. <https://doi.org/10.1016/j.btre.2017.02.006>.
34. Kannan RRR, Arumugam R, Ramya D, Manivannan K, Anantharaman P. Green synthesis of silver nanoparticles using marine macroalgae *Chaetomorpha Linum*. *Appl Nanosci (Switzerland).* 2013;3:229–33. <https://doi.org/10.1007/s13204-012-0125-5>.
35. Souza TGF, Ciminelli VST, Mohalleh NDS. A comparison of TEM and DLS methods to characterize size distribution of ceramic nanoparticles. *J Phys Conf Ser.* 2016;733. <https://doi.org/10.1088/1742-6596/733/1/012039>.
36. Filippov SK, Khusnutdinov R, Murmiliuk A, Inam W, Zakharova LY, Zhang H, Khutoryanskiy VV. Dynamic light scattering and transmission electron microscopy in drug delivery: A roadmap for correct characterization of nanoparticles and interpretation of results. *Mater Horiz.* 2023;10:5354–70. <https://doi.org/10.1039/D3MH00717K>.
37. Sathiyaseelan A, Saravanakumar K, Mariadoss AVA, Wang MH. Biocompatible fungal chitosan encapsulated phytochemical silver nanoparticles enhanced antidiabetic, antioxidant and antibacterial activity. *Int J Biol Macromol.* 2020;153:63–71. <https://doi.org/10.1016/j.ijbiomac.2020.02.291>.
38. Manikandaselvi S, Sathya V, Vadivel V, Sampath N, Brindha P. Evaluation of bio control potential of AgNPs synthesized from *trichoderma viride*. *Adv Nat Sci NanoSci NanoTechnol.* 2020;11:035004. <https://doi.org/10.1088/2043-6254/a/b9d16>.
39. Shettar SS, Bagewadi ZK, Yunus Khan TM, Mohamed Shamsudeen S, Kolvekar HN. Biochemical characterization of immobilized recombinant subtilisin and synthesis and functional characterization of recombinant subtilisin capped silver and zinc oxide nanoparticles. *Saudi J Biol Sci.* 2024;31:104009. <https://doi.org/10.1016/J.SJBS.2024.104009>.
40. Sharma I, Gupta P, Kango N. Synthesis and characterization of keratinase laden green synthesized silver nanoparticles for valorization of feather keratin. *Sci Rep.* 2023;13:1. <https://doi.org/10.1038/s41598-023-38721-6>.
41. Wang X, Lee SY, Akter S, Huq MA. Probiotic-mediated biosynthesis of silver nanoparticles and their antibacterial applications against pathogenic strains of *Escherichia coli* O157:H7. *Polymers.* 2022;14:1834. <https://doi.org/10.3390/POLYM14091834>.
42. Vala AK, Trivedi H, Gosai H, Panseriya H, Dave B. Biosynthesized silver nanoparticles and their therapeutic applications. *Compr Anal Chem.* 2021;94:547–84. <https://doi.org/10.1016/BS.COAC.2020.12.010>.
43. Ershov VA, Ershov BG. Effect of silver nanoparticle size on antibacterial activity. *Toxics.* 2024;12:801. <https://doi.org/10.3390/TOXICS12110801/S1>.
44. Taghavizadeh Yazdi ME, Nourbakhsh F, Mashreghi M, Mousavi SH. Ultrasound-based synthesis of ZnO-Ag₂O₃ nanocomposite: Characterization and evaluation of its antimicrobial and anticancer properties. *Res Chem Intermed.* 2021;47:1285–96. <https://doi.org/10.1007/S11164-020-04355-W/FIGURES/7>.
45. Arun Subash H, Santhosh K, Kannan K, Pitchiah S. Extraction of keratin degrading enzyme from marine actinobacteria of *nocardia* Sp and their antibacterial potential against oral pathogens. *Oral Oncol Rep.* 2024;9:100184. <https://doi.org/10.1016/J.OOR.2024.100184>.
46. Yazdi MET, Darroudi M, Amiri MS, Hosseini HA, Nourbakhsh F, Mashreghi M, Farjadi M, Kouhi SMM, Mousavi SH. Anticancer, antimicrobial, and dye degradation activity of biosynthesized silver nanoparticle using *Artemisia kopetdaghensis*. *Micro Nano Lett.* 2020;15:1046–50. <https://doi.org/10.1049/MNL.2020.0387>.
47. Characterization of *Aspergillus flavus* NG 85 laccase and its dye decolorization efficiency, (n.d.). https://www.researchgate.net/publication/312913538_Characterization_of_Aspgillus_flavus_NG_85_laccase_and_its_dye_decolorization_efficiency (accessed February 13, 2025).
48. Rawat D, Mishra V, Sharma RS. Detoxification of azo dyes in the context of environmental processes. *Chemosphere.* 2016;155:591–605. <https://doi.org/10.1016/J.CHEMOSPHERE.2016.04.068>.
49. Tomar R, Abdala AA, Chaudhary RG, Singh NB. Photocatalytic degradation of dyes by nanomaterials. *Mater Today Proc.* 2020;29:967–73. <https://doi.org/10.1016/J.MATPR.2020.04.144>.
50. Dadashi J, Ali Ghasemzadeh M, Alipour S, Zamani F. A review on catalytic reduction/degradation of organic pollution through silver-based hydrogels. *Arab J Chem.* 2022;15:104023. <https://doi.org/10.1016/J.ARABJC.2022.104023>.
51. Jyoti K, Singh A. Green synthesis of nanostructured silver particles and their catalytic application in dye degradation. *J Genetic Eng Biotechnol.* 2016;14:311–7. <https://doi.org/10.1016/J.JGEB.2016.09.005>.
52. Faheem M, Riaz A, Alam M, Wahad F, Sohail M, Altaf M, Abbas, 2D nanostructured MXene-Based Silver Nanoparticles for Photocatalytic Degradation of Safranin Dye. *Catalysts.* 2024;14:201. <https://doi.org/10.3390/CATAL14030201/S1>.
53. Afzal MA, Javed M, Aroob S, Javed T, Alnoman MM, Alelwani W, et al. The biogenic synthesis of bimetallic Ag/ZnO nanoparticles: A multifunctional approach for methyl violet photocatalytic degradation and the assessment of antibacterial, antioxidant, and cytotoxicity properties. *Nanomaterials.* 2023;13:2079. <https://doi.org/10.3390/NANO13142079/S1>.
54. Es-haghi A, Amiri MS, Taghavizadeh ME, Yazdi. Ferula latisepta gels for synthesis of zinc/silver binary nanoparticles: antibacterial effects against gram-negative and gram-positive bacteria and physicochemical characteristics.

BMC Biotechnol. 2024;24:1–17. <https://doi.org/10.1186/S12896-024-00878-X/FIGURES/9>.

55. Abd El-Ghany MN, Hamdi SA, Korany SM, Elbaz RM, Emam AN, Farahat MG. Microorganisms Biogenic Silver Nanoparticles Produced by Soil Rare Actinomycetes and Their Significant Effect on Aspergillus-derived Mycotoxins. *Microorganisms*. 2023;11:1006. <https://doi.org/10.3390/microorganisms11041006>
56. Khalil NM, Abd El-Ghany MN, Rodríguez-Couto S. Antifungal and anti-mycotoxin efficacy of biogenic silver nanoparticles produced by *Fusarium*

chlamydosporum and *Penicillium chrysogenum* at non-cytotoxic doses. *Chemosphere*. 2019;218:477–86. <https://doi.org/10.1016/J.CHEMOSPHERE.2018.11.129>.

Publisher's note

Springer Nature remains neutral with regard to jurisdictional claims in published maps and institutional affiliations.